TECHNICAL DIVISION
SAVANNAH RIVER LABORATORY

Received by OSTI
MAY 2 9 1990

DPST-71-317

DISTRIBUTION:

J. W. Croach -
A. A. Johnson, Wilm.
D. F. Babcock -
J. S. Neill
W. P. Bebbington, SRP
L. W. Fox
E. O. Kiger
W. M. Olliff
A. H. Peters
D. A. Ward -
R. H. Towell
C. H. Ice -
L. H. Meyer, SRL
S. Mirshak
F. D. King
G. F. Merz
E. Wingo
H. Knoebel
S. Durant
H. Baker
J. Brown
A. Willis
R. Taylor
D. Harris
Crain, Jr.
P. Morin
R. Muhlbaier
W. Ridenhour, Jr.
TIS File Copy
Vital Records File

M E M O R A N D U M

DPST--71-317

DE90 011240

TO: J. M. BOSWELL

FROM: M. W. HODGES MWH

EFFECT OF RIB ON BURNOUT HEAT FLUX

INTRODUCTION

Ribs contacting the surfaces of reactor assemblies insulate the surface and cause local reductions in coolant velocity resulting in local heat flux perturbations. These perturbations can be represented as a reduction in the burnout heat flux for surfaces contacted by a spacer rib as compared to an ideal surface, i. e., no rib present. This memorandum presents results of burnout tests with insulating ribs on aluminum surfaces and proposes a method for applying the results to reactor assemblies.

SUMMARY

Burnout heat flux was measured for vertical aluminum heaters that were locally insulated by vertical ribs and cooled on one side by downward flowing water. Results of these tests were correlated by the following equation:*

$$\left[\left(\frac{Q}{A}\right)_{BO}\right]_{RIB} = \left[0.687-11.655\left(\frac{X_o}{\sqrt{ky}}\right)\right]\left[\left(\frac{Q}{A}\right)_{BO}\right]_{IDEAL} \quad (1)$$

$$0.001 \le \frac{X_o}{\sqrt{ky}} \le 0.009$$

*Equation 1 should not be extrapolated beyond the $X_o/\sqrt{ky}$ values indicated.

where

$\left[\left(\frac{Q}{A}\right)_{BO}\right]_{RIB}$ = average heat flux from a surface contacted by a rib when the burnout conditions are reached, pcu/ft^2-hr,

$\left[\left(\frac{Q}{A}\right)_{BO}\right]_{IDEAL}$ = burnout heat flux without ribs, pcu/ft^2-hr, = 102,400 (1+0.0515V)(1+0.124 T_{sub}) for aluminum surfaces,

X_o = (width of rib tip)/2, ft,

k = thermal conductivity of heated surface or for a fuel element, the cladding, pcu/ft^2-hr-°C/ft,

y = thickness of heater of half thickness of tubes or heaters cooled from both sides, ft,

V = velocity, ft/sec

T_{sub} = subcooling, °C

The data are summarized in Table I and Figure 3.

The standard deviation of the data from the correlation was 6.5%. Because the 3σ value (19.5%) and estimated maximum experimental error (21.1%) are approximately the same, Equation (1) can be used directly without an additional uncertainty factor to calculate the nonideality factor for rib contact.

The nonideality factors for the rib effect calculated by the following two equations should be used in $BOSF_N$ limit calculations:

for $y \leq 0.0109$ and $0.001 \leq \frac{X_o}{\sqrt{ky}} \leq 0.009$.

$$H_{RIB} = \frac{\left[\left(\frac{Q}{A}\right)_{BO}\right]_{RIB}}{\left[\left(\frac{Q}{A}\right)_{BO}\right]_{IDEAL}} = 1.0-12.53(y)^{0.56}\left\{0.313+11.655\left(\frac{X_o}{\sqrt{ky}}\right)\right\} \quad (2)$$

for $y > 0.0109$,

$$H_{RIB} = 0.687-11.655\left(\frac{X_o}{\sqrt{ky}}\right) \quad (3)$$

where H_{RIB} is the nonideality factor to account for the effect of rib contact on the burnout heat flux.

Equation (2) accounts for the relative heat split for heat generated under an insulated rib for a heater cooled from both sides. For thick tubes or slugs (>0.0218-ft thick), the rib affects the burnout heat flux only on the side contacted by the rib; hence, Equation (3) is applicable. The nonideality factors calculated using the above equations are applicable to all current SRP fuel and target assemblies and varies from 0.84 for the Mark 18 to 0.66 for the Mark 30D.

DISCUSSION

A rib contacting the surfaces of fuel tubes or target slugs or target tubes reduces the burnout heat flux in two ways. The rib acts as an insulator over part of the surface causing a localized increase in heat flux in the region adjacent to the rib. The rib also causes a reduction in the mean coolant velocity in the region adjacent to the rib which reduces the heat removing capacity of the coolant adjacent to the rib.

Burnout tests utilizing aluminum strip heaters and nonconducting ribs have been conducted in the heat transfer laboratory of SRL and at Columbia University. Figure 1 is a sketch of the test rig cross section at SRL. Three aluminum strips, 0.62-0.65-inch wide and 19.25-inches long were placed side by side on a "transite" backup plate and the aluminum strips were electrically connected in series. The coolant channel was 2.05-inches wide and from 0.23 to 0.25-inch thick. Heater thickness was varied from 0.030 to 0.060 inch and rib widths were varied from 0 to 0.250 inch. Zero rib width was achieved by placing the rib on one side of the channel and butting it against the edge of the heater. Heater geometry may have affected the data slightly because of the gaps between strips which provided breaks in the conduction path as well as convective cooling zones at the edges of the strips; however, these effects should be slight since the width to thickness ratio is large and effects of perturbations in local heat flux become negligible beyond about 3 or 4 heater thicknesses from the perturbation.

The cross section of the Columbia University test rig is shown in Figure 2. The heater strip, which was 2-inches wide, 0.060-inch thick, and 6-feet long, was cooled from two sides by water flowing in 0.25-inch thick channels. A 0.060-inch nonconducting rib was centered in one channel and contacted the heater over its entire length. The primary uncertainties in the Columbia tests were concerned with possible flow between the channels and accuracy of measured pressures. A small leak was discovered in the manifold system for the pressure instrumentation after the conclusion of the tests. Results of burnout tests for both SRL and Columbia University are given in Table I and Figure 3. The Columbia results shown are based on flows and temperatures measured in the channel with the rib.

The results for zero rib width were not included in the correlation. However, these results do indicate that even though a portion of the heater is not insulated by rib contact there is a reduction in the burnout heat flux caused by velocity effects due to the rib boundary to the channel. The appropriate non-ideality factor for the velocity effect for heaters cooled from both sides is discussed in more detail later.

In some tests, the heaters failed due to melting under the ribs, i.e., the centerline temperature under the rib exceeded the melting point in attempting to fin heat to adjacent areas. This occurred for $X_o/\sqrt{ky} > 0.009$ indicating that the thermal properties of the heater were limiting rather than the local burnout heat flux adjacent to the rib. A similar phenomenon was reported in DP-562[1] for stainless steel heaters and $X_o/\sqrt{ky} > 0.02$.

Because of the possibility of lack of contact between the rib and heater, tests in which the reductions from the ideal burnout heat flux were less than that predicted by the correlation with 3σ values were not included in the correlation.

In addition to measuring reductions in burnout heat flux, special tests were conducted to investigate the mechanisms involved in burnout adjacent to rib insulated surfaces. Videotapes were made of burnout tests with ribs located both in the center and at one side of the channel. Bulk flow in the vertical test section was downward with a velocity of 20 ft/sec; however, prior to burnout, local flow reversal was observed in a narrow region (0.25 to 0.5-inch wide) next to the rib. The upflow was accompanied by the formation of thin films, apparently on the heater surface, which moved upward slowly. Burnout was approached by holding the mean flow, pressure, and heat flux constant while the coolant temperature was increased gradually. Finally, just prior to burnout, the vapor films would slow and burnout would result when one film remained over a section of heater long enough to raise the temperature of the heater to the melting point. With a 0.060-inch thick heater, a 0.125-inch rib, and a surface heat flux of 1×10^6 pcu/ft^2-hr, the film remained stationary approximately 0.3 sec before burnout occurred. The adiabatic heating time for the heater was calculated to be 0.25 sec, which agrees well with the observed film residence time. The films were estimated to be approximately 0.25-inch wide.

With ribs located in the center of the channel, thermocouples were placed under the rib near the expected burnout point. As shown in Figure 4, as the local flow reversal phenomenon developed, a large increase was observed in the temperature under the rib. This is probably due to the formation of a narrow vapor film next to the rib. This film is sustained adjacent to the rib, stably, for a long period of time (>20 sec). This is because the drag forces acting on the film are not as large as in the free stream and the heat generated both under the rib and under the film can be removed by heat conduction to adjacent surfaces and from these surfaces to the coolant. The film noted in the previous discussion as remaining on the surface for 0.3 sec was further removed from the rib (0.25 to 0.3 in) and led to melting. Up to the burnout point, vapor films cannot be stably maintained away from the rib. The actual indicated temperature may be slightly in error due to calibration inaccuracies and extraneous signals from the voltage drop across the junction, but the temperature trend is real.

Results of burnout tests with ribs on stainless steel surfaces and applicable nonidealities are reported in DP-562. When these results are applied to heaters cooled from both sides, only 50% of the measured reduction in burnout heat flux for heaters cooled from one side was used. Very thick tubes or tubes with low thermal conductivity may not conduct as much of the heat generated under the rib to the side opposite the rib as thin tubes; therefore, some other criterion is required to determine the applicability of results obtained on heaters cooled on one side to tubes cooled on both sides.

The fraction of the rib factor for heaters cooled from one side applicable to a surface of a tube cooled from both sides should be related to the relative division of the heat not leaving the area contacted by the rib to either side of the tube just prior to burnout. The TOAD code was used to calculate the relative heat splits for various geometries. The TOAD code is a two-dimensional (r and θ) conduction code with surface temperature dependent heat transfer coefficients. The heat flux perturbation for the Mark 16 with an insulated rib is shown in Figure 5. Calculations for all current assemblies are summarized in Figure 6. The percentage of the heat generated under the rib which is distributed to the surface contacted by the rib was determined to be only a slight function of the thermal conductivity and can be conservatively calculated as

$$\text{RSHFP} = 1253 \cdot (y)^{0.58}, \quad y \leq 0.0109 \text{ ft} \tag{4}$$

where

RSHFP = rib side heat flux perturbation, % of total heat generated under rib which would normally be convected from the area contacted by the rib.

Equation (4) is valid only for $y \leq 0.0109$ ft. Equation (4) is combined with Equation (1) to give Equation (2). For half thicknesses greater than 0.0109 ft, the total reduction in the burnout heat flux determined from heaters cooled on one side should be used.

The hydrodynamic effect of the rib on burnout heat flux is apparent from the tests with zero rib width and the local upflow phenomena observed just prior to burnout. The increased temperature under the rib prior to burnout (Figure 4) and the local flow reversal phenomenon indicate that sufficient time is available such that the heater would attempt to redistribute the heat under the rib to the surface opposite the rib. This is verified by the

Columbia University results, i.e., the reduction from the ideal burnout heat flux is less than predicted by Equation (2). The calculated reduction in burnout heat flux for the geometry run at Columbia University using Equation (2) is 16.1%. This compares with 11.6% and 9.5% measured in the two tests. It seems reasonable to assume that the hydrodynamic perturbation of the burnout heat flux would be distributed approximately the same as the perturbation caused by the insulating effect. Hence, as the two effects are combined in the experimental data correlated by Equation (1), Equation (2) distributes them similarly in determining the applicable nonideality factor.

Stainless steel data from DP-562 are compared with Equation (1) in Figure 7. Reductions from the ideal correlation are similar to aluminum results; however, the absolute magnitude of the burnout heat fluxes are about 20% less. For assemblies with both core and cladding with low thermal conductivities, the aluminum burnout heat flux correlation is not applicable and the results of DP-562 as summarized in Figure 7 should be used. Because the aluminum burnout correlation is based on tests with 0.020-inch heaters, it is applicable to all assemblies with aluminum cladding thicknesses equal to or greater than 0.020 inch regardless of the core conductivity. Hence, Equation (2) and (3) should be used with the aluminum correlation with all current SRP fuel and target assemblies. The results in DP-562 and the stainless steel burnout correlation are applicable only to stainless steel or zirconium clad fuel assemblies.

MWH:nmg
Attach. (8)

REFERENCE

[1] S. Mirshak and R. H. Towell. Heat Transfer Burnout of a Surface Contacted by a Spacer Rib. DP-562, April 1961.

TABLE I

BURNOUT DATA FOR RIBS ON ALUMINUM SURFACES

Run No.	X_o, ft	y, ft	$X_o/\sqrt{ky}$	V, ft/sec	T_{SUB}, °C	P, psia	$\phi_{Meas.}$ $\times 10^{-6}$	ϕ_{Ideal} $\times 10^{-6}$	% Reduction	Comparison with Correlation: $(\phi_{Rib}/\phi_{Ideal})$ Meas.	Comparison with Correlation: $(\phi_{Rib}/\phi_{Ideal})$ Correlation	Comparison with Correlation: % Difference	Comment
B01	0.0	.00516	0.0	18.3	34.0	56.0	1.10	1.04	-5.7	-	-	-	A
B02	.00291	"	.00365	18.2	47.1	55.7	.896	1.359	34.1	.659	.661	0.3	
B03	.00291	"	.00365	14.9	53.7	53.9	.913	1.389	34.2	.658	.661	0.5	
B04	.00133	"	.00166	19.8	59.7	55.2	1.035	1.738	40.4	.596	.715	16.6	
B05	.00133	"	.00166	18.8	48.4	55.7	1.037	1.412	26.6	.734	.715	-2.7	
B06	.00062	"	.00079	17.6	48.6	57.7	1.073	1.375	22.0	-	-	-	C
B07	.00520	"	.00651	17.3	77.2	53.7	.888	2.046	56.6	-	-	-	B
B08	.00533	"	.00666	18.1	58.0	54.2	.882	1.619	45.5	.545	.622	12.4	
B09	0.0	"	0.0	18.5	42.3	54.7	1.178	1.248	5.6	-	-	-	A
B10	.00125	"	.00156	17.6	58.0	54.7	1.062	1.602	33.7	.663	.719	7.8	
B11	.00266	"	.00333	19.3	52.1	54.7	.915	1.521	39.8	.602	.667	9.7	
B12	.00062	"	.00079	18.1	39.5	55.1	1.038	1.166	11.0	-	-	-	F
H00	.0025	.0025	.00449	16.25	48.8	54.7	.885	1.326	33.3	.667	.647	-3.1	
H01	.00063	.0025	.00115	19.2	79.4	54.7	1.415	2.190	54.7	-	-	-	D
H02	0.0	.00417	0.0	19.2	39.5	54.7	1.028	1.202	14.5	-	-	-	E
H03	.00542	.0025	.00754	19.9	43.7	58.2	1.020	1.328	23.2	.768	.615	-24.9	F
H04	0.0	.00417	0.0	21.2	38.7	58.2	1.071	1.242	13.8	-	-	-	E
H05	0.0	"	0.0	20.7	34.0	57.5	.971	1.104	12.0	-	-	-	E
H06	.00542	"	.00754	19.8	50.9	53.2	.992	1.512	34.4	.656	.615	-6.7	
H07	.0025	"	.00353	18.3	33.7	55.5	.992	1.030	3.7	-	-	-	G
H08	0.0	"	0.0	17.3	31.2	55.0	1.062	.943	-12.6	-	-	-	E
H09	0.0	"	0.0	22.7	50.0	54.0	1.107	1.599	30.7	-	-	-	E
H10	.0025	"	.00348	19.6	48.3	54.7	1.015	1.438	29.4	.706	.664	-6.3	
H11	.0025	"	.00348	22.8	50.9	59.7	1.006	1.628	38.2	.618	.664	6.9	
H12	.0050	"	.00696	21.7	52.1	54.1	.983	1.616	34.3	.608	.620	1.9	
H13	.00521	"	.00725	23.0	58.3	55.7	1.062	1.841	42.3	.577	.617	6.5	
H14	.00521	"	.00725	22.9	48.9	59.7	1.014	1.575	35.6	.644	.617	-4.4	
H15	.00521	.0025	.00951	20.3	73.6	61.7	1.000	2.199	52.8				B
H16	.01040	.0025	.0190	26.5	94.5	55.7	1.028	2.920	64.8				B
H17	.00521	.0025	.00951	25.0	58.2	57.4	.999	1.925	48.1				B
CU1	0.0	.0025	0.0	15.4	96.5	64.7	.361	2.377	84.8				H
CU2	0.0	.0025	0.0	16.1	34.7	64.7	1.002	.994	-0.9				
CU3	.0025	.0025	.00449	15.2	37.8	68.7	.916	1.037	11.6				
CU4	.0025	.0025	.00449	15.5	37.7	69.7	.946	1.045	9.5				

A - not used in correlation; no rib.
B - not used in correlation; melting under rib.
C - not used in correlation; burnout not next to rib.
D - not used in correlation: apparent heater defect.
E - not used in correlation: zero rib width
F - not used in correlation; greater than 3 σ deviation.
G - not used in correlation; short in bus.
H - burnout at bus.
ϕ - burnout heat flux, pcu/ft²-hr.

FIGURE 1

HEATER CONFIGURATION AND
CHANNEL GEOMETRY, SRL TESTS

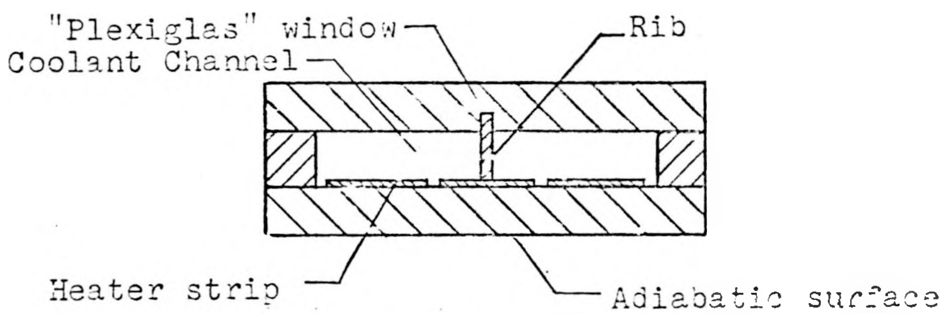

(A)

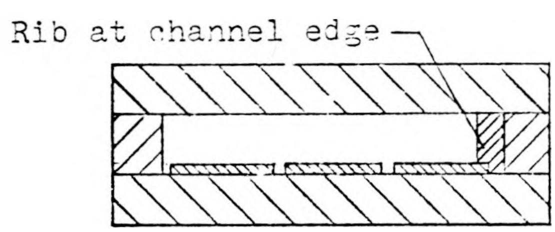

(B)

FIGURE 2

COLUMBIA UNIVERSITY TEST RIG

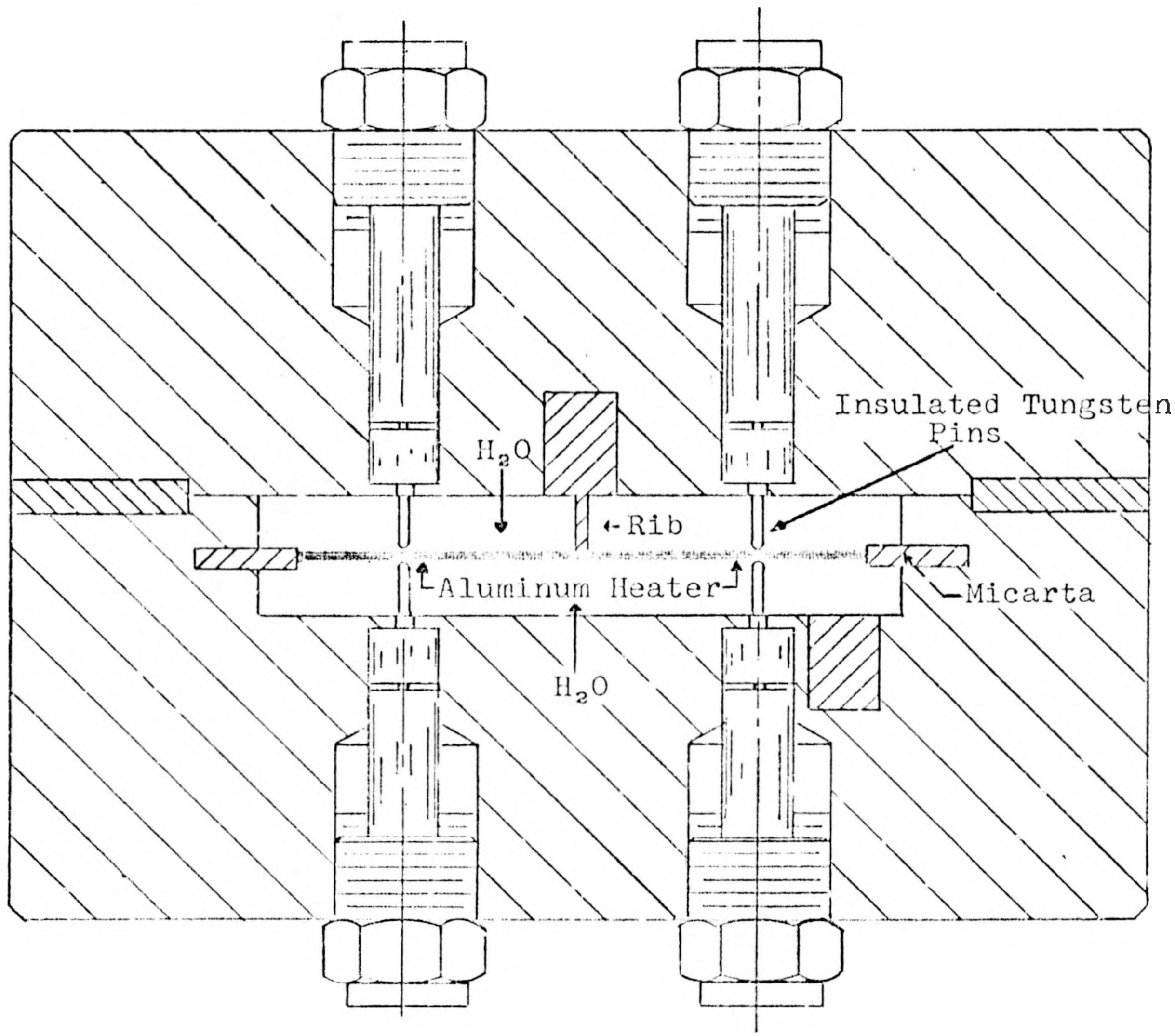

FIGURE 3

EFFECT OF RIB ON BURNOUT HEAT FLUX

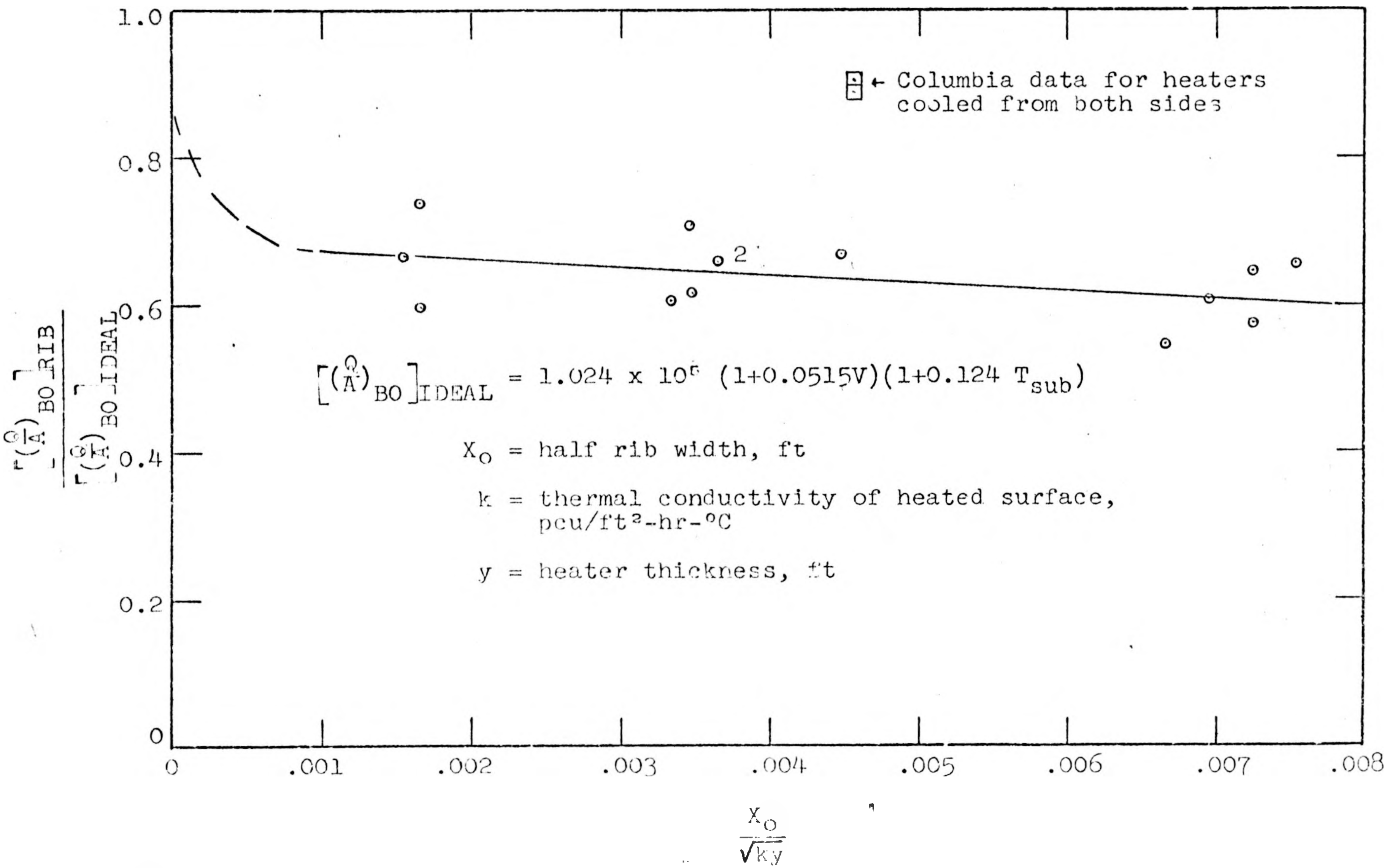

FIGURE 4

INDICATED TEMPERATURE UNDER 1/8 in.
RIB NEAR BURNOUT POINT

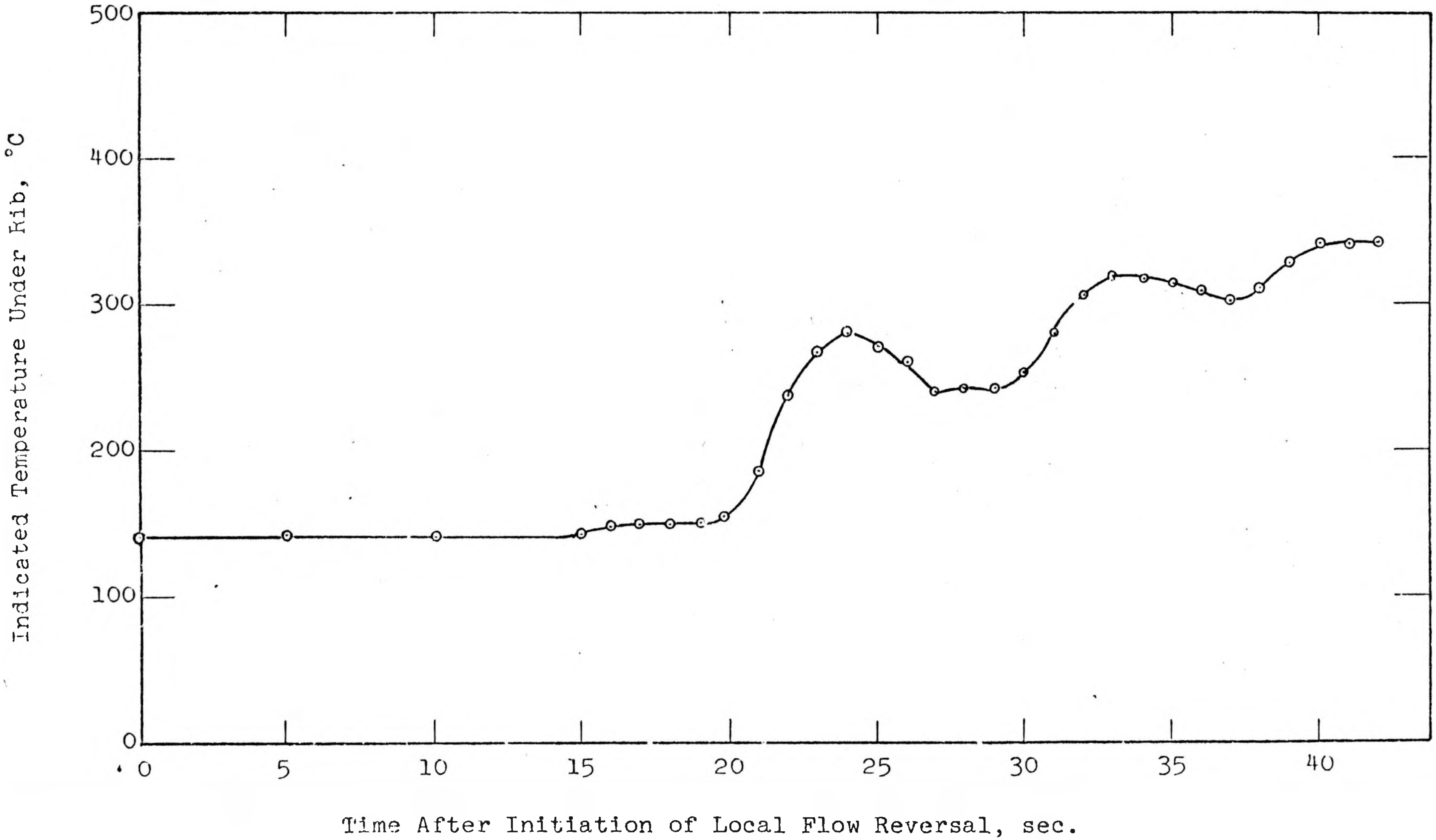

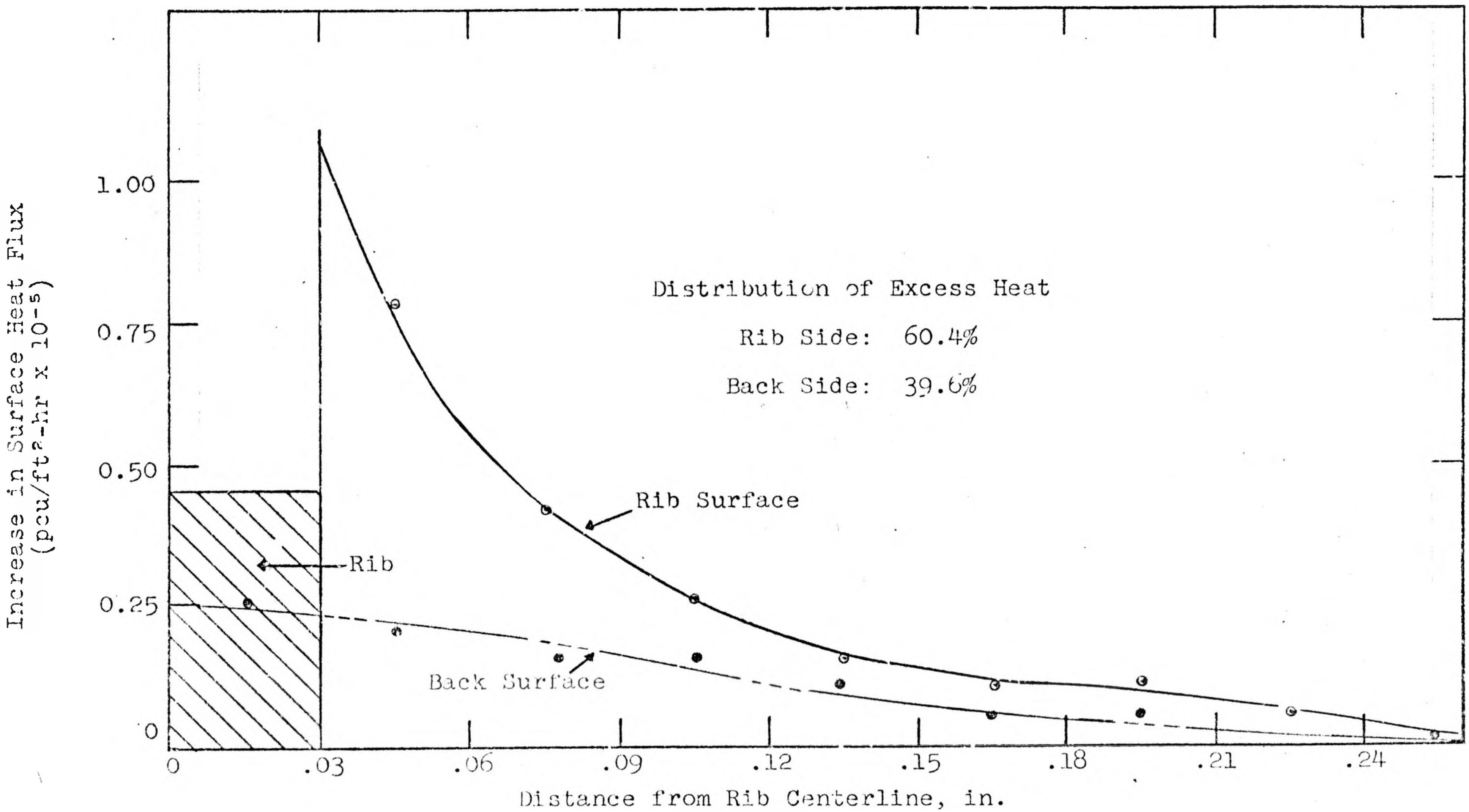

FIGURE 5

LOCAL INCREASE IN SURFACE HEAT FLUX DUE TO PRESENCE OF INSULATING RIB, MK 16, 30-MIL CLADDING

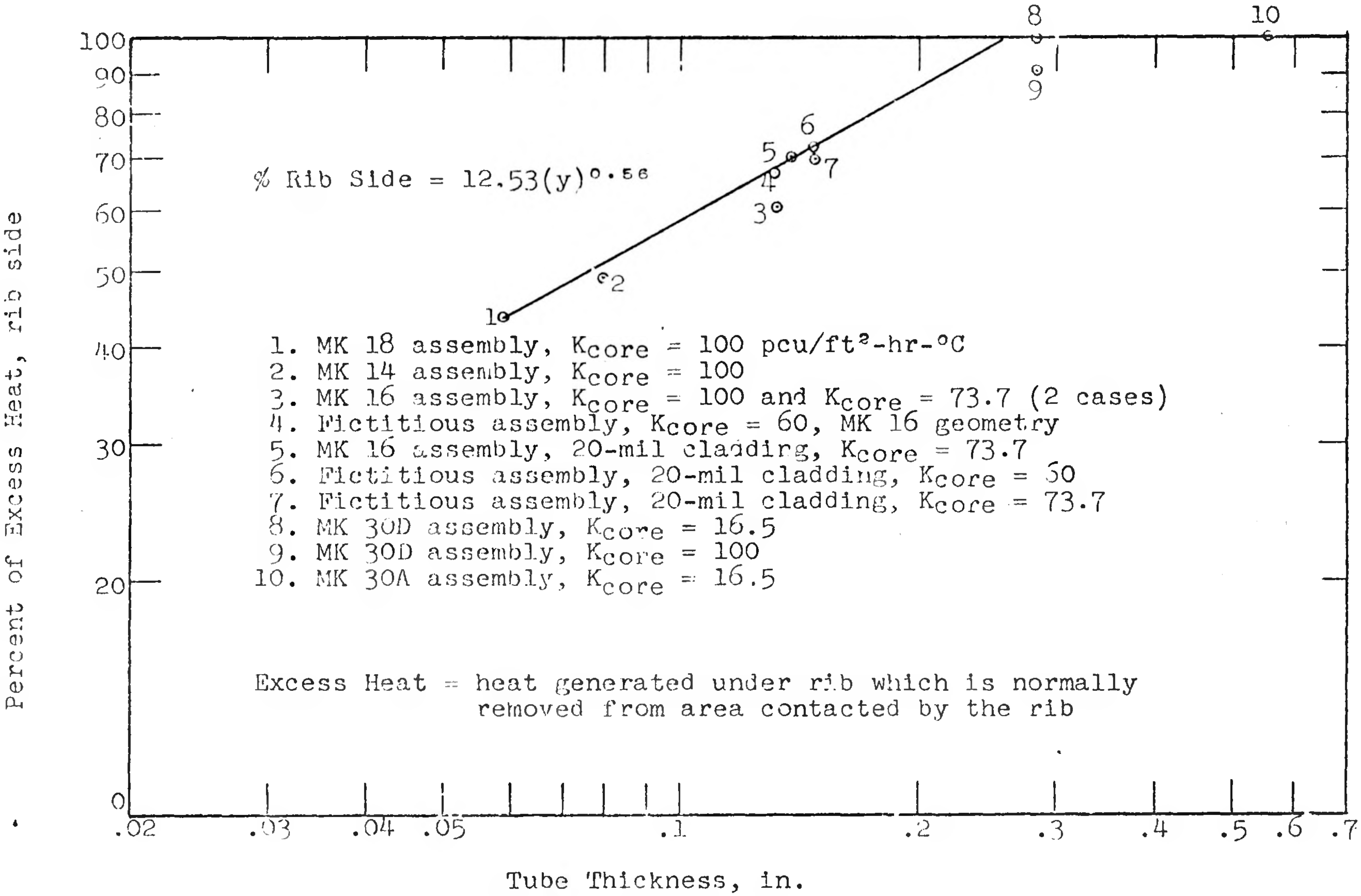

FIGURE 6

DISTRIBUTION OF EXCESS HEAT GENERATED UNDER RIB TO RIB INSULATED SURFACE (TOAD CODE RESULTS)

FIGURE 7

COMPARISON OF STAINLESS STEEL DATA FROM DP-562 WITH EQUATION 1